Scientia Iranica D (2021) 28(6), 3437–3449

SCIENTIA IRANICA

Sharif University of Technology
Scientia Iranica
Transactions D: Computer Science & Engineering and Electrical Engineering
http://scientiairanica.sharif.edu

Estimation of solar energy generation in an 80 kW station in Kabudrahang, Iran: A comparative study

R. Kazemi Golkhandan[a], H. Torkaman[b,*], and A. Keyhani[c]

a. *Faculty of Electrical & Computer Engineering, University of Birjand, Birjand, Iran.*
b. *Faculty of Electrical Engineering, Shahid Beheshti University, A.C., Tehran, Iran.*
c. *Department of Electrical and Computer Engineering, Ohio State University, Ohio, USA.*

Received 21 January 2019; received in revised form 12 February 2019; accepted 6 May 2019

KEYWORDS
Solar generating station;
Boost converter;
Inverter;
Maximum power point;
Photovoltaic model.

Abstract. Estimation of solar energy generation using integrated power systems must be performed for power systems in terms of long-term planning and short-term control. Irradiation is one of the main factors affecting the resulting energy of any solar system. Hence, investigation of solar irradiation on the horizontal surface facilitates proper and efficient implementation of a solar energy system. Capturing much more energy from irradiation through Photovoltaic (PV) cells results in the enhancement of energy generation in PV station. The present paper aims to study the effectiveness of applying two topologies to energy harvesting in PV stations. The topologies include (a) PV station with multilevel boost converters and inverters and (b) PV station with only multilevel inverters. This study investigated an 80 kW PV test station, located in Kabudrahang, Iran. The comparison of the results pointed to the effectiveness of multilevel converters in the output of PV arrays in harvesting a significant volume of solar energy. Simulation results showed that the results of utilizing the proposed topology in harvesting the maximum power from a PV station were promising.

1. Introduction

Due to growing demand for installation of Photovoltaic (PV) capacity in the world, the concept of Maximum Power Point (MPP) tracking has been developed for PV systems [1]. MPP tracking is an essential component of PV systems. This scheme ensures that the system can always harvest maximum power regardless of environmental changes, namely ambient temperature and solar insolation [2]. Several MPP tracking techniques and their application were reported in [3,4]. Since the Power-Voltage (P-V) characteristic curve varies nonlinearly with solar irradiation and atmospheric temperature conditions, tracking MPP was a challenge, though successfully achieved using several methods presented in [5,6].

In order to calculate the output power of a PV station, it is of significance to take the environmental parameters, irradiation, and temperature into consideration [7,8]. Since irradiation and temperature vary during the day, they must be studied as functions of time. Irradiation on a particular day depends on the angle that the sun makes with the PV panels, air mass, and cloud cover [9]. In [10], prediction of daily global solar irradiation was performed using temporal Gaussian process regression. In [11], a methodology was proposed to choose a representative daily-duration irradiance signal based on long-term irradiance data.

In case of the unavailability or shortage of relevant

*. *Corresponding author. Tel.: +98 21 73932525*
E-mail addresses: reza.kazemi@birjand.ac.ir (R. Kazemi Golkhandan); H_torkaman@sbu.ac.ir (H. Torkaman); keyhani1@osu.edu (A. Keyhani)

doi: 10.24200/sci.2019.52667.2826

data on irradiation, some approaches can be employed to estimate it based on single PV module output parameters. In [12], a closed-form analytical estimator for the irradiation based on measurements of the DC voltage, current, and cell temperature and a model of PV arrays were proposed. Similarly, in [13], a globally convergent estimator based on Immersion and Invariance (I&I) principle was presented. In [14], solar irradiation forecasting was performed using artificial neural network and random forest methods. In [15], temperature and DC electrical measurements were used to perform real-time estimation of irradiation. The main drawback of this system is that it moves in three different states (panel underload, short circuit, and open circuit) which is a feature not typically implemented in commercial PV systems. Therefore, the knowledge of irradiation and temperature plays an essential role in investigating the output parameters of PV systems. In [16], both the estimation and validation of daily global solar irradiation by day-of-the-year-based models were investigated for different climates. Besides, validity and effectiveness of the ensemble technologies and hybrid methods were determined. In [17], a novel approach to estimation of monthly average daily solar radiation with its complex spatial pattern through machine learning techniques was developed.

A PV station consists of PV modules in which a number of PV cells are connected in series. A number of PV modules connected in series form a string and a number of strings connected in parallel form arrays. Series and parallel connections would accordingly increase the voltage and current ratings of the PV system [18].

Since both irradiation and temperature determine the output voltage of PV arrays, they make PV systems intermittent, unpredictable, and unreliable [19]. Irradiation directly affects the output voltage of a PV cell and temperature inversely affects the output voltage. As irradiation goes up and temperature goes downs in an allowable range, the output voltage of PV cell increases, and vice versa.

Power electronic converters, applied to the PV stations, are capable of operating at a certain level of voltage. This fact limits the harvested output power of PV systems during operation in case of low irradiation and high temperature. In such conditions, the power electronic inverter in the PV system would not be capable of converting DC to AC power at the required voltage level. Regardless of variations in irradiation and temperature, MPPT and voltage regulation can be achieved by implementing high-ratio DC-DC converters [20,21] which would result in the efficiency improvement of the PV system. In [22], an MPP tracking algorithm based on Monod Equation, used for estimating the output power for each current output of the PV station, was proposed to estimate the required duty cycle for the converter in the PV system.

In this paper, first, a model of the PV module was extracted. Then, two cases of a typical PV station with a capacity of 80 kW in Kabudrahang, Iran were illustrated and studied in detail. One case referred to the time when PV arrays were directly connected to the power grid through multilevel inverters. The inverters were used in the PV station to change the DC output voltage of PV arrays at the grid AC voltage level. The other case pointed to the time when multilevel boost converters and inverters were utilized in the PV station. Applying boost converter to increase the output voltage level of PV cells made it feasible to reach the cut-off voltage of the inverter. Much more power was harvested during the operation of the PV station with proper coordination of converters and PV station voltage output. Input data of irradiation and temperature profiles in the location of the PV station were collected from practical measurements. Simulations were performed to study the effectiveness of the proposed strategy for the 80 kW PV station.

2. Model of PV module

To design a PV station, first, a PV source model should be extracted. In this regard, a Single-Diode Model (SDM) of PV module with series and parallel resistances was considered, as shown in Figure 1 [7].

SDM consists of a current source, a diode, and series and parallel resistances. The voltage-current $(V - I)$ relationship of PV can be written based on Kirchhoff's current law [23] as follows:

$$I = I_{ph} - I_o \left(\exp \left(\frac{V + R_s I}{n_s . V_t} \right) - 1 \right) - \frac{V + R_s I}{R_p}, \tag{1}$$

where V is the module output voltage and I is the output current. I_{ph} and I_o are the photogenerated and dark saturation currents, respectively. V_t is the junction thermal voltage. R_s and R_p are the series and parallel resistances, respectively. n_s is the number of series-connected cells in the module. In addition, V_t

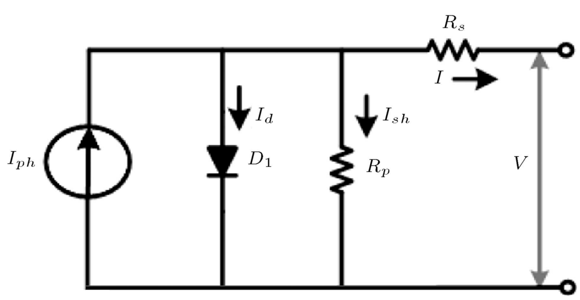

Figure 1. Single-diode model of PV module with series and parallel resistances.

is the thermal voltage of a diode and is expressed as follows:

$$V_t = \frac{KTA}{q}, \tag{2}$$

where K is Boltzmann's constant, T is the junction temperature in Kelvin, A is the diode ideality factor, and q is the electronic charge. The model presented in Figure 1 incorporates five unknown parameters based on (1): I_{ph}, I_o, V_t, R_s, and R_p. The information provided in the manufacturer's datasheet shows that I_{sc}, V_{oc}, V_{mpp}, and I_{mpp} in the module are short circuit current, open circuit voltage, voltage at MPP, and current on MPP, respectively. Moreover, the temperature coefficients for short-circuit current K_i and open-circuit-voltage K_v were already determined in the datasheets. The objective of PV modeling was to estimate the model parameters under Standard Test Conditions (STC) in different environmental conditions using the datasheet information provided by the module manufacturer. The parameter estimation was done based on the numerical methods such as Gauss-Seidel. $(0, I_{sc})$, (V_{mpp}, I_{mpp}), and $(V_{oc}, 0)$ represent the specified points on the $(V - I)$ curve, facilitating the estimation of the parameters. In [24], parameter estimation of PV cells was performed through some selected evolutionary algorithms using datasheet information at three major points of V–I characteristics. In [25], Maximum Likelihood Estimator (MLE) and Newton Raphson (NR) resolution were proposed to identify unknown parameters of single-diode PV module in different test conditions.

In this respect, to simplify Eq. (1), the term "–1" was neglected against the exponential term for convenience. Eqs. (3)–(5) are obtained by substituting the values of remarkable points into Eq. (1):

$$I_{sc} = I_{ph} - I_o \left(\exp\left(\frac{R_s.I_{sc}}{n_s.V_t} \right) \right) - \frac{R_s.I_{sc}}{R_p}, \tag{3}$$

$$I_{mpp} = I_{ph} - I_o \left(\exp\left(\frac{V_{mpp} + R_s.I_{mpp}}{n_s.V_t} \right) \right) - \frac{V_{mpp} + R_s.I_{mpp}}{R_p}, \tag{4}$$

$$0 = I_{ph} - I_o \left(\exp\left(\frac{V_{oc}}{n_s.V_t} \right) \right) - \frac{V_{oc}}{R_p}. \tag{5}$$

In order to estimate these five unknown parameters, in addition to the aforementioned Eqs. (3)–(5), two other equations are needed.

First, since the derivative of PV output power with respect to PV voltage is zero at MPP, Eq. (6) is appropriate for estimating unknown parameters:

$$\frac{dP}{dv}(V = V_{mpp}, I = I_{mpp}) = 0. \tag{6}$$

Table 1. Datasheet values and estimated parameters of a Mitsubishi module.

Datasheet parameters		Estimated parameters	
I_{SC}	7.36 A	I_{ph}	7.36 A
V_{OC}	30.4 V	I_0	0.104 μA
V_{mpp}	24.2 V	A	1.310
I_{mpp}	50	R_s	0.251 Ohm
n_s	50	R_{sh}	1168 Ohm
Temperature coefficients			
K_i	0.057%	K_v	–0.346%

Second, the slope of $V - I$ characteristic at short-circuit point, which is calculated using Eq. (7) [26], can be regarded as another equation for estimating unknown parameter.

$$\frac{dI}{dv}(V = 0, I = I_{sc}) = -\frac{1}{R_{sh0}}. \tag{7}$$

This paper employed Mitsubishi Electric PV-MF165EB3 module as test PV module. Table 1 shows the values provided in the module datasheet followed by the values for the unknown parameters estimated through the Gauss-Seidel method [7].

3. PV station with boost converter and inverter

To harvest the maximum available power using a PV station, a boost converter is applied to the system to step up the output voltage of the PV arrays in case of low irradiation and high temperature. Implementing this approach would increase the value of output voltage to more than the cut-off voltage of the inverter. Therefore, the inverter starts operating at these moments that were not able to operate when PV station was equipped only with the inverter. The output voltage of a boost converter in the PV system is calculated in Eq. (8) [27,28]:

$$V_{dc} = \frac{V_{pv}}{1 - D}, \tag{8}$$

where D is the duty ratio of the power electronic switch in the converter. Eq. (8) is based on the continuous mode of conductance. Thus, the current of the inductor in the converter cannot be zero during operation. As mentioned in [26], the limit for the continuous mode of converter conduction can be written in Eq. (9) [29]:

$$I_{PV} = \frac{\Delta I_L}{2}, \tag{9}$$

where I_{PV} and ΔI_L are the average values of the inductor current from the output of the PV arrays and the peak-to-peak variation, respectively. Eq. (10) demonstrates how the value of peak-to-peak voltage variation is calculated in the boost converter [27].

$$\Delta I_L = \frac{V_{PV}.D}{f.L}. \tag{10}$$

By substituting the value of ΔI_L in Eq. (10), from Eq. (9), the duty ratio can be calculated in Eq. (11):

$$D = \frac{2.I_{PV}.L_{\min}.f_s}{V_{PV}}, \tag{11}$$

where $L_{\min}$ represents the minimum value of the inductance that ensures the continuous mode of operation.

As depicted in Eq. (11), duty ratio depends on the values for the voltage and current of PV arrays, inductance of the converter, and switching frequency. The value of duty ratio is limited by the parameters mentioned here. According to Eq. (11), for a limited value of duty ratio, the output voltage of the converter would be limited, too. In this condition, the output voltage of the converter would not be sufficient to be applied to the inverter. Finally, the PV system cannot provide the grid with the required power due to the insufficient output voltage of the converter, and it limits the output power of the PV system in low-irradiation and high-temperature conditions.

To resolve this problem, converters with lower step-up voltage should be proposed to harvest power at lower voltage levels. Therefore, the overall efficiency of the system would increase.

3.1. PV station with inverter

When PV arrays are directly connected to the inverter, the output voltage of PV arrays must be above the cut-off value for initialization of the inverter operation. In this condition, space vector modulation is applied to produce the output voltage of the inverter. The output voltage of the inverter is related to its input voltage, applied from PV arrays, determined by the modulation index. This index varies between zero and one. The output line-to-line voltage of the inverter can be calculated as follows [27]:

$$Vi_{L-L} = \frac{V_{dc}}{\sqrt{2}} \cdot M_a. \tag{12}$$

The grid voltage determines the output voltage of the inverter, maintained by the grid, and it should remain constant. Therefore, during variations in the output voltage of PV arrays, modulation index variation facilitates achieving a constant voltage in the inverter output. The minimum value of the voltage of PV arrays can be calculated, considering that $M_a = 1$. Thus, the minimum value of DC voltage can be calculated as follows:

$$V_{dc,\min} = \sqrt{2} \cdot Vi_{L-L}. \tag{13}$$

Similar to the previous section, during the day when the output voltage of PV arrays falls below a certain level, called the cut-off voltage, the inverter would not operate. Therefore, to harvest the maximum power as the output, the PV arrays must be connected to an inverter with a lower cut-off voltage.

3.2. Formulation of irradiation on the PV arrays

To perform calculations, the irradiation on the PV panels must be calculated. The irradiation on a horizontal surface is calculated as follows [30]:

$$I_{hor} = S.E_o \cdot [\cos\delta \cdot \cos(\varphi-\beta)\cos\omega + \sin\delta \cdot \sin(\varphi-\beta)], \tag{14}$$

where S is the solar constant and defined as the rate of energy received by a unit area perpendicular to the rays at a distance of one astronomical unit. The value of solar constant is 1367 W.m^{-2} [31]. E_o is the eccentricity correction factor of the earth's orbit and is calculated for each day of the year, as shown in the following [32]:

$$E_o = 1 + 0.033\cos\left(\frac{2\pi d_n}{365}\right), \tag{15}$$

where d_n is the day number of the year. δ is the declination angle and is calculated by Eq. (16), which is an empirical formula [33]:

$$\delta = 23.45\sin\left[\frac{360(d_n + 284)}{365}\right]. \tag{16}$$

φ is the latitude the location, ω is the solar hour angle, and β is the tilt angle. Detection of the optimum value of the tilt angle was studied in [34].

Eq. (14) is used to calculate the irradiation on the surface outside the earth's atmosphere. A fraction of this irradiation reaches the surface of the earth due to the diffusion of rays and their absorption into the atmosphere.

4. Case study statement

In this paper, a 80 kW PV station as the test system was investigated. Of note, each solar PV array is a combination of some modules first connected in series to achieve the desired voltage and then, connected in parallel to allow the system to produce the desired current.

The values for the photo-generated and dark saturation current in the module and string are the same, but those of the series and parallel resistances are different and must be calculated. For the 80 kW arrays consisting of PV-MF165EB3 modules, as shown in Table 1, with 15 modules per string and 32 strings

Table 2. Calculation of parameters for the 80 kW PV station.

$n_s = 15 - n_p = 32$		
Equivalent 80 kW PV arrays parameters		Relationship with module parameters
I_{ph}	235.57 A	$I_{ph} \times n_p$
I_0	3.314 A	$I_0 \times n_p$
A	1.310 A	A
R_s	0.117 Ohm	$R_s \times n_s/n_p$
R_{sh}	547.77 Ohm	$R_{sh} \times n_s/n_p$

in parallel, the estimated parameters are extracted, the results of which are shown in Table 2. In this table, n_p is the number of modules connected in parallel in an array.

In both topologies, PV arrays were directly connected to the inverter through DC-DC boost converter and implemented on the considered test system, the results of which are demonstrated in the next section. Multilevel inverters were utilized in the proposed topology. As mentioned earlier, irradiation and temperature at the location of the PV arrays determine the output voltage level of the PV arrays. When the irradiation level is high and the temperature is low, converters with higher voltage levels are employed. Conversely, when the irradiation level is low and temperature is high, converters with lower voltage levels are used. Figure 2(b) shows topology two when the PV arrays are connected to the inverter through DC/DC boost converter. This topology enjoys a boost converter which provides a stable and high voltage for the inverter. Therefore, the inverter is rated at a lower current rating at the same power level. Multilevel converters were implemented in the proposed topology that yielded much more energy harvesting during working conditions because when the voltage of the PV arrays was not sufficient for the inverter to operate, a boost converter was used to step up the voltage of PV arrays to a value above the lower cut-off voltage for the inverter.

The topology shown in Figure 2(a) enjoys lower cost because the cost of using the boost converter is not considered. Figure 2(b) presents the second topology that benefits from the boost converter, providing a stable and high voltage for the inverter.

In both topologies, the line-to-line output voltage of the inverter has a square shape. To omit the harmonics and extract a sinusoidal AC voltage, suitable to be injected into the power grid, LC filters were applied to a point at which the inverters were connected to the power grid. Application of the delta-wye connection of the transformer helps trap the third harmonic of voltage and provide the null point for the network.

The values for the parameters including voltage, current, and power in the output of a PV system depend on temperature and irradiation at the location of the PV arrays. To investigate how these values were affected by temperature and irradiation, a sample day in a year, i.e., 5th of October at 10:10 am, was considered. Figure 3(a)–(d) demonstrate how voltage-current-output power, when applying two topologies, change with temperature and irradiation variations.

Figure 3(a) shows that while increasing the irradiation at a fixed temperature, the output voltage of PV arrays increases. At a fixed irradiation level, upon increase in the temperature, the value of the output voltage of PV arrays would decrease. The maximum value for the output voltage of PV arrays is 448.92 V. Figure 3(b) indicates that increasing the irradiation and decreasing the temperature would result in increasing the level of output current. The maximum value of the resulting current of PV arrays is 160 A. Figure 3(c) and (d) show the output power of the PV station using the two mentioned topologies. Obviously, after applying the boost DC/DC converter to the output of PV arrays, the harvested energy would increase. Boost converter would enhance the output voltage level to values higher than the cut-off voltage level of the inverter.

5. Simulation and implementation results and analysis

In this study, a one-year period was considered to perform the simulation. The results obtained from this simulation were used to compare these two topologies. Specific days in weeks, Wednesdays in this respect, were selected as the sample days. The profiles of irradiation and temperature at the location of PV station, Kabudrahang, were extracted from practical measurements.

Irradiation at the location of the PV station during the year under study is given in Figure 4. The maximum value of the energy from irradiation at the location of the station was 8.6 kWh per day. Figure 5 illustrates temperature profile at the location of the PV station. The minimum and maximum values of the measured temperatures were –9.94 and 30.47, respectively.

Latitude longitude coordinates of Kabudrahang are 35.21°N and 48.72°E. Tilt angle is 30° [34]. Following the application of Eqs. (15) and (16), E_0 and δ were calculated for the Wednesdays of a year with the resulting values listed in Table 3.

Irradiation, voltage, and current profile of the mentioned PV system during sampling day hours of the summer quarter are given in Figure 6(a) to (c).

As depicted in Figure 6(a), irradiations on the PV arrays vary during times of the days. Maximum values of irradiation on the Wednesdays of the summer

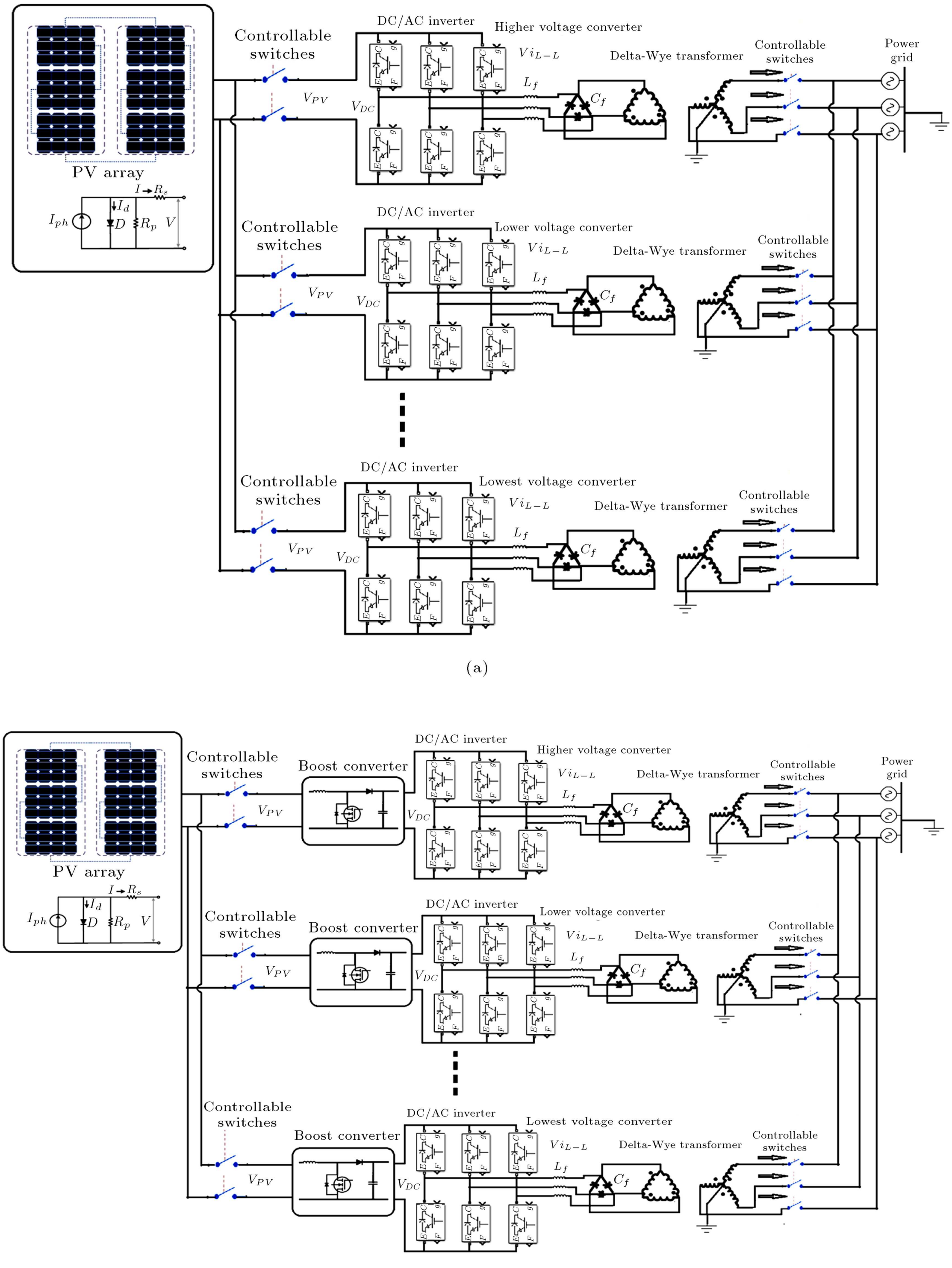

Figure 2. Topology of the PV station connected to the grid: (a) Topology 1: PV arrays directly connected to the inverter and (b) Topology 2: PV arrays connected to the inverter through a boost converter.

quarter vary between 846.91 and 1038.6 watts per square meters. Maximum value, 1038.6 watts per square meters, occurs on the 7th Wednesday of the summer quarter. Minimum values of irradiation on the Wednesdays of the summer quarter vary between 1 and 4.22 watts per square meters. Minimum values occur upon sunrise and sunset. Here, the minimum value, 1 watt per square meters, occurs on the 5th Wednesday of the summer quarter. Regarding the irradiation profile over the 13 weeks of the summer quarter, as depicted

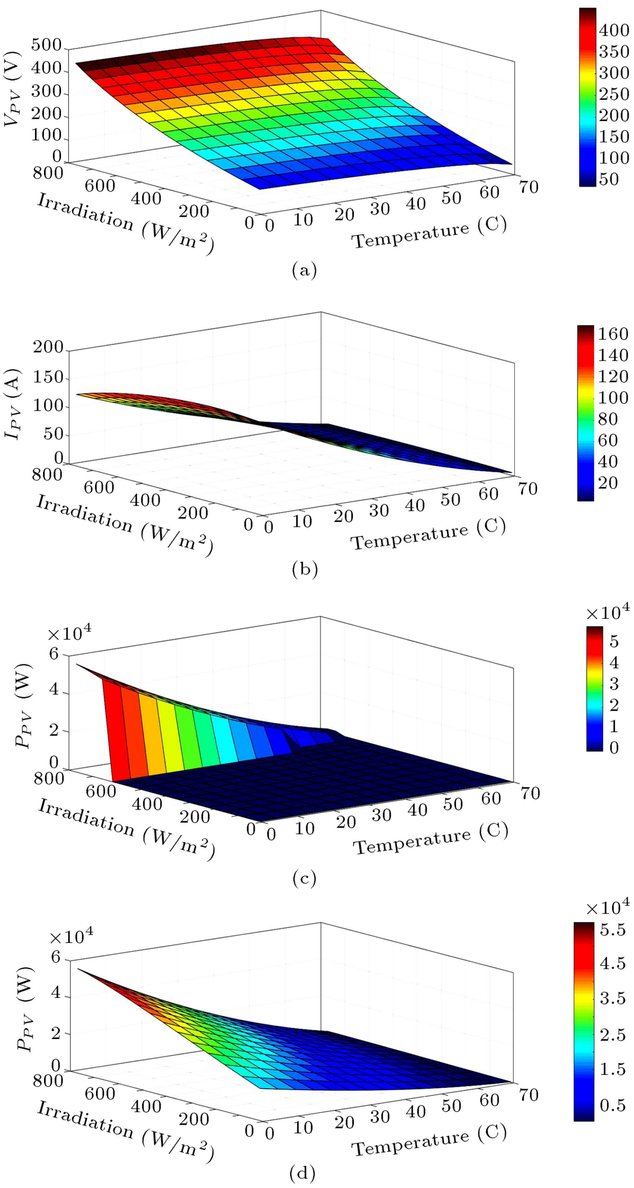

Figure 3. Voltage, current, and power output of 80 kW PV station with and without a boost converter as a function of irradiation and temperature: (a) PV voltage, (b) PV current, (c) PV output power without boost converter, and (d) PV power output with a boost converter.

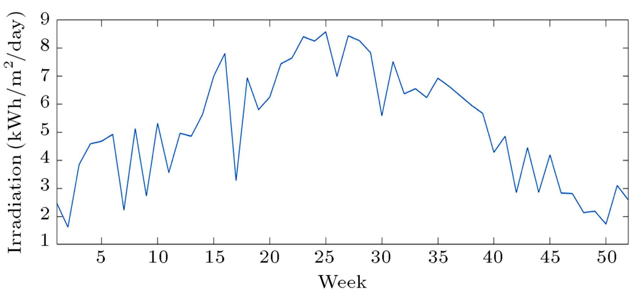

Figure 4. Irradiation received by an 80-kW generating station located in Kabudrahang, Iran for the weeks through a year.

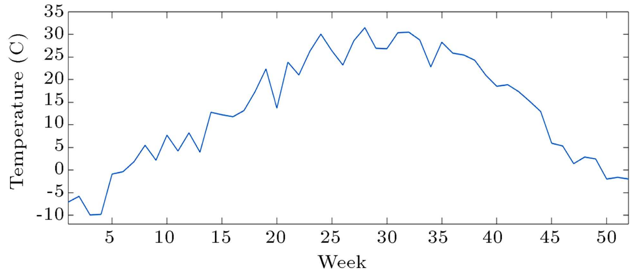

Figure 5. The environmental temperature profile of an 80 kW generating station located in Kabudrahang, Iran for the weeks through a year.

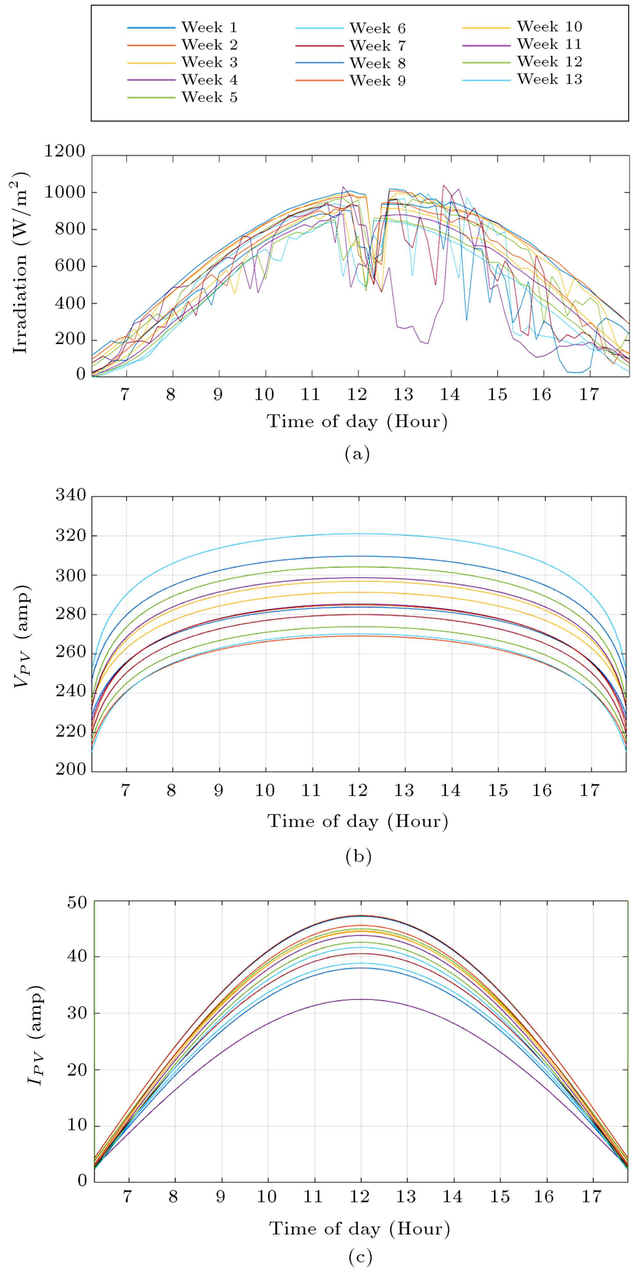

Figure 6. (a) Irradiation, (b) voltage, and (c) current profile of 80 kW PV station in Kabudrahang, Iran for the summer quarter.

Table 3. Values of eccentricity correction factor of the earth's orbit and declination angle for the Wednesdays under study.

Day	**Jan 5**	**Jan 12**	**Jan 19**	**Jan 26**	**Feb 2**	**Feb 9**	**Feb 16**	**Feb 23**	**Mar 2**	**Mar 9**	**Mar 16**	**Mar 23**	**Mar 30**
E_0	1.033	1.032	1.031	1.030	1.028	1.025	1.023	1.019	1.016	1.013	1.009	1.005	1.001
δ	–22.6	–21.7	–20.5	–19.0	–17.2	–15.2	–12.9	–10.5	–7.9	–5.2	–2.4	0.4	3.2
Day	**Apr 6**	**Apr 13**	**Apr 20**	**Apr 27**	**May 4**	**May 11**	**May 18**	**May 25**	**Jun 1**	**Jun 8**	**Jun 15**	**Jun 22**	**Jun 29**
E_0	0.997	0.993	0.989	0.985	0.982	0.979	0.976	0.973	0.971	0.969	0.968	0.967	0.966
δ	6.0	8.6	11.2	13.6	15.8	17.7	19.5	20.9	22.0	22.8	23.3	23.4	23.2
Day	**Ju 16**	**Jul 13**	**Jul 20**	**Jul 27**	**Aug 3**	**Aug 10**	**Aug 17**	**Aug 24**	**Aug 31**	**Sep 7**	**Sep 14**	**Sep 21**	**Sep 28**
E_0	0.966	0.967	0.968	0.969	0.971	0.974	0.976	0.979	0.983	0.986	0.990	0.994	0.998
δ	22.7	21.8	20.8	19.1	17.3	15.3	13.1	10.7	8.1	5.4	2.6	–0.2	–3.0
Day	**Oct 5**	**Oct 12**	**Oct 19**	**Oct 26**	**Nov 2**	**Nov 9**	**Nov 16**	**Nov 23**	**Nov 30**	**Dec 7**	**Dec 14**	**Dec 21**	**Dec 28**
E_0	1.002	1.006	1.010	1.014	1.017	1.020	1.023	1.026	1.028	1.030	1.031	1.032	1.033
δ	–5.8	–8.5	–11.0	–13.4	–15.6	–17.6	–19.3	–20.8	–21.9	–22.8	–23.3	–23.4	–23.2

in Figure 6(a), the output voltage of the PV arrays can be calculated, as given in Figure 6(b). The line-to-line voltage of the power grid was 240 volts in the simulation. According to Eq. (13), the minimum value of dc voltage in the input of the inverter must be 340 volts to initialize the inverter operation. Given that the output voltage of PV arrays in the summer quarter does not reach this value, the inverter would not start operating. Figure 7(a) illustrates this fact. For energy harvesting, the boost converter was added to the PV station. In the case of applying a boost converter, its output voltage was preserved at 480 V DC, with a switching frequency of 5 KHz and inductance of 5 mH, while the output voltage of the inverter was preserved at 240 V AC. This would result in energy harvesting during the summer quarter, as depicted in Figure 7(b).

To make a comparison between the two cases, the output power profiles of a PV system with only a boost converter and a PV system with boost converter and inverter were studied, as shown in Figure 7.

To make a numerical comparison between the two cases, the daily output energy of PV station with the inverter and output energy of PV station with boost converter and inverter, during 13 Wednesdays of the summer quarter, was calculated, as mentioned in Table 4. The application of the boost converter to the output of PV arrays helps increase the output energy harvesting. The maximum value of the output energy was 228.2 kWh, which was attained on the 4th Wednesday of the summer quarter. The minimum value of the output energy was 99.008 kWh attained during the 13th Wednesday of the summer quarter.

The procedure described above was repeated for the autumn quarter, and the results were given below. Irradiation, voltage, and current profile of the mentioned PV system during sampling day hours of the autumn quarter are given in Figure 8(a) to (c).

Like the previous section, as depicted in Figure 8(a), irradiations on the PV arrays vary during certain time intervals of the days. Maximum irradiation values on the Wednesdays of the autumn quarter

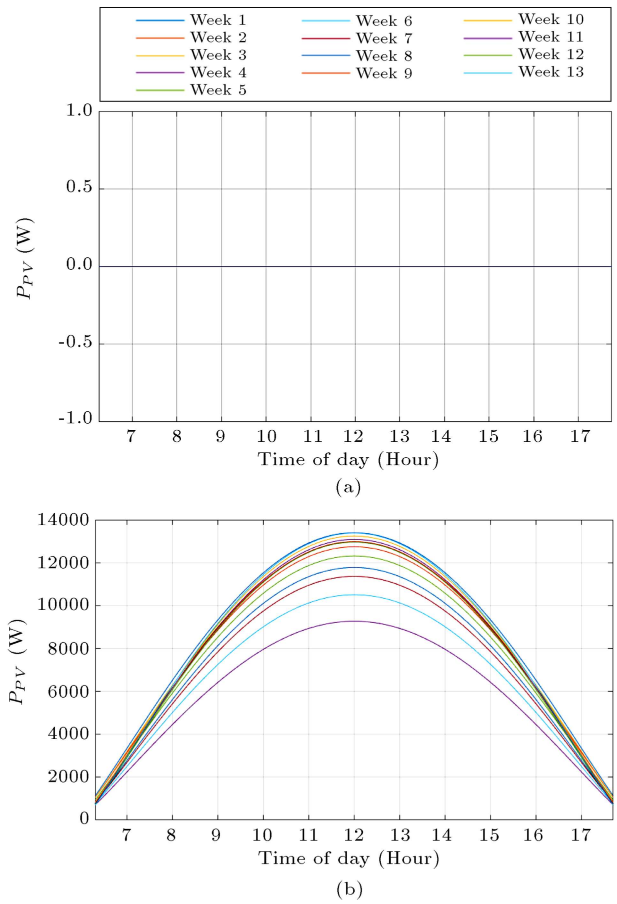

Figure 7. (a) Output power of PV station with an only inverter and (b) Output power of PV station with a boost converter and an inverter.

Table 4. The output energy of PV station during days of summer quarter when applying two topologies with: (a) only an inverter and (b) a boost converter and an inverter.

Day	The output energy of PV station with an inverter (kWh/day)	The output energy of PV station with boost converter and inverter (kWh/day)	Max. value of output voltage (Volt)	Day	The output energy of PV station with an inverter (kWh/day)	The output energy of PV station with boost converter and inverter (kWh/day)	Max. value of output voltage (Volt)
1	0	152.19	283.77	**8**	0	145.68	309.56
2	0	143.37	269.04	**9**	0	147.37	284.83
3	0	150.67	291.22	**10**	0	152.08	296.87
4	0	228.20	285.31	**11**	0	151.03	298.64
5	0	140.91	273.80	**12**	0	151.13	304.16
6	0	126.66	270.14	**13**	0	99.008	320.97
7	0	135.05	279.92				

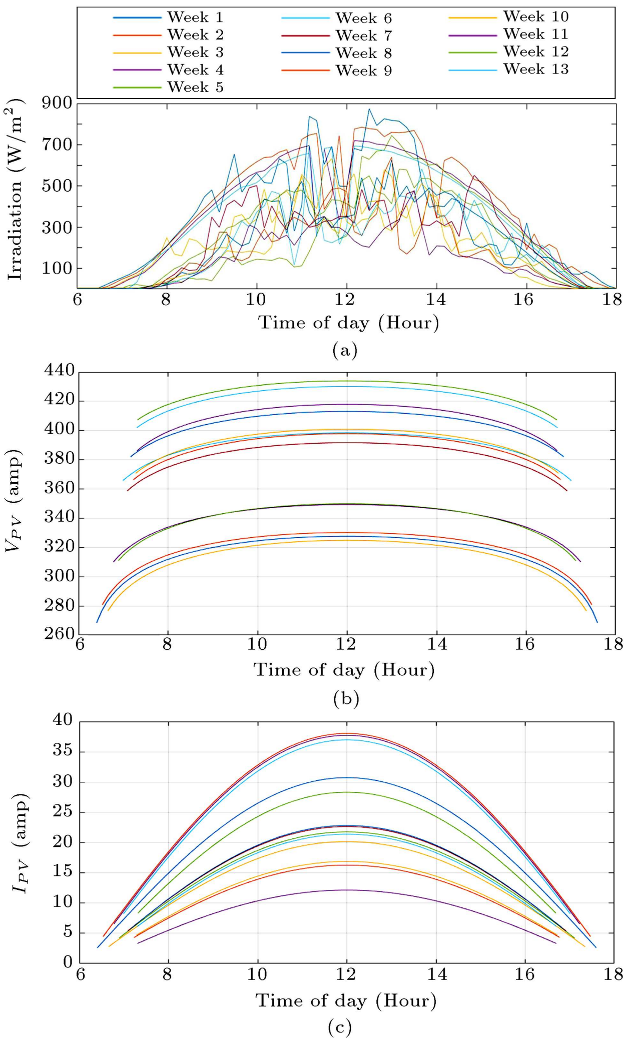

Figure 8. (a) Irradiation, (b) voltage, and (c) current profile of 80 kW PV station in Kabudrahang, Iran for autumn quarter.

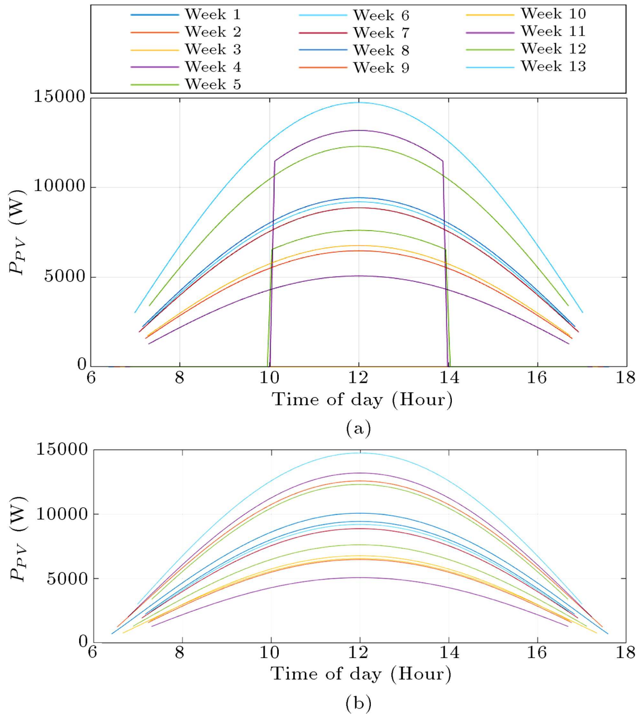

Figure 9. (a) Output power of PV station with an only inverter and (b) output power of PV station with a boost converter and an inverter.

varied from 477.66 to 874.67 watts per square meters. Maximum value, 874.67 watts per square meters, was reached on the 1st Wednesday of the autumn quarter. Minimum irradiation values on the Wednesdays of the autumn quarter varied from 1 to 2 watts per square meters. Here, the minimum value, 1 watt per square meters, was reached on the 13th Wednesday of the autumn quarter.

Here, like the previous section, regarding the irradiation profile in the 13 weeks of the autumn quarter, as depicted in Figure 8(a), the output voltage of the PV arrays can be calculated in Figure 8(b). To make a comparison between the two cases, the output power profile of the PV system with only a boost converter and that of the PV system with a boost converter and an inverter are given in Figure 9.

Table 5. The output energy of PV station during days of autumn quarter when applying two topologies with (a) only an inverter and (b) a boost converter and an inverter.

Day	The output energy of PV station with an inverter (kWh/day)	The output energy of PV station with boost converter and inverter (kWh/day)	Max. value of output voltage (Volt)	Day	The output energy of PV station with an inverter (kWh/day)	The output energy of PV station with boost converter and inverter (kWh/day)	Max. value of output voltage (Volt)
1	0	74.021	327.65	**8**	66.368	66.368	413.06
2	0	92.111	330.23	**9**	45.140	45.140	397.87
3	0	47.450	324.88	**10**	47.025	47.025	401.00
4	48.611	95.555	349.34	**11**	34.985	34.985	417.92
5	28.852	54.557	349.90	**12**	85.670	85.670	433.94
6	105.52	105.52	398.44	**13**	63.972	63.972	430.20
7	62.793	62.793	391.71				

To make a numerical comparison between the two cases, like the previous section, the daily output energy of the PV station with an inverter and the output energy of the PV station with a boost converter during the 13th Wednesdays of the autumn quarter were calculated, as mentioned in Table 5. In some cases, the output voltage of PV arrays was below the cut-off voltage for initialization of the inverter and the output energy of PV station with the only inverter was zero. The maximum value of the output energy was 105.52 kWh, which was obtained during the 6th Wednesday of the autumn quarter. The minimum value of the output energy was 34.985 kWh which was obtained during the 11th Wednesday of the autumn quarter.

The output power of the PV station located in Kabudrahang, Iran, 35°N and 48°E, varies in different days of a year according to irradiation and weather conditions. As mentioned in Figure 3, for summer months, the available power produced at the PV station involving only an inverter is zero as the output voltage of PV panels is less than the cut-off value, 340 V DC determined by Eq. (6). The output power of the PV station increased when applying a DC-DC boost converter before using the inverter because this procedure lengthens the harvesting time of solar beam energy from sunrise to sunset, except a few minutes after sunrise and before sunset.

Clear skies during months of autumn, without overcast, with medium ambient temperatures, help achieve much energy from the PV station.

Figure 10 shows the total harvested solar energy during specific days, Wednesdays, in the weeks of a year. As shown, the energy production level of the PV station when equipped with a boost converter and an inverter was much more than the condition with only an inverter.

As mentioned above, the output voltage of the PV arrays depends on the level of irradiation and temperature. Low voltage levels in the output of PV arrays cannot be applied to the inverter as they are below the cut-off voltage level. To produce power from PV arrays, separate boost converter and inverter sets with lower voltage ratings are required. Here, another solution to the case of study was designed. The voltage of the boost converter was reduced from 480 V DC to 240 V DC, and the voltage of the inverter was reduced from 240 V AC to 120 V AC. This reduction in voltage levels would result in achieving much more power as the output of the PV station. Table 6 shows additional energy output in kWh on different days of the year when the voltage of the boost converter was reduced from 480 V DC to 240 V DC and the inverter voltage was reduced from 240 V AC to 120 V AC.

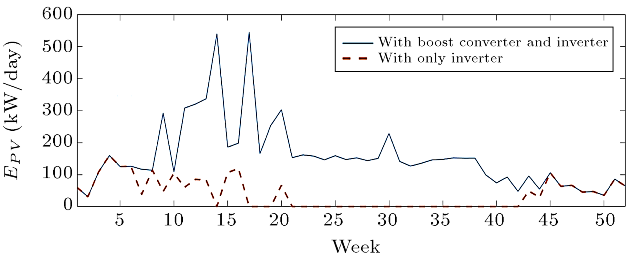

Figure 10. Additional energy output from an 80 kW PV station in kWh in Kabudrahang, Iran on different days of the year when the voltage of the boost converter is reduced from 480 V DC to 240 V DC and the inverter voltage is reduced from 240 V AC to 120 V AC.

According to the results shown in Table 6, Figure 11 shows the concluded graph of the captured energy difference in the case of applying two topologies when the voltages of the boost converter and inverter were reduced from 480 V DC to 240 V DC and from 240 V AC to 120 V AC, respectively.

According to Figure 10, the additionally produced energy when the voltages of the boost converter and inverter were reduced from 480 V DC to 240 V DC and from 240 V AC to 120 V AC in the PV system

Table 6. The energy output from an 80 kW PV station in kWh in Kabudrahang, Iran on different days of the year when the voltage of the boost converter is reduced from 480 V DC to 240 V DC and the inverter voltage is reduced from 240 V AC to 120 V AC.

Day	**Jan 5**	**Jan 12**	**Jan 19**	**Jan 26**	**Feb 2**	**Feb 9**	**Feb 16**	**Feb 23**	**Mar 2**	**Mar 9**	**Mar 16**	**Mar 23**	**Mar 30**
MPPT with B & I	0	0	0	0	0	0	78.5	0	245	4.4	247.4	235	254
MPPT with I	0	0	0	0	0	0	0	0	0	0	0	0	0
Day	**Apr 6**	**Apr 13**	**Apr 20**	**Apr 27**	**May 4**	**May 11**	**May 18**	**May 25**	**Jun 1**	**Jun 8**	**Jun 15**	**Jun 22**	**Jun 29**
MPPT with B & I	539.6	79.8	78.5	545.2	165	253	236	153	161.5	157.7	145.9	159	147
MPPT with I	0.14	0.16	0	0	0.14	0	0	0.13	0.14	0	0	0	0.12
Day	**Jul 6**	**Jul 13**	**Jul 20**	**Jul 27**	**Aug 3**	**Aug 10**	**Aug 17**	**Aug 24**	**Aug 31**	**Sep 7**	**Sep 14**	**Sep 21**	**Sep 28**
MPPT with B & I	152.2	143.4	150.7	228.2	141	126.8	135.2	145.8	147.4	152.1	151	151.1	99
MPPT with I	0	0	0	0	0	0.11	0.11	0.12	0	0	0	0	0
Day	**Oct 5**	**Oct 12**	**Oct 19**	**Oct 26**	**Nov 2**	**Nov 9**	**Nov 16**	**Nov 23**	**Nov 30**	**Dec 7**	**Dec 14**	**Dec 21**	**Dec 28**
MPPT with B & I	74	92	47.5	47	25.7	0	0	0	0	0	0	0	0
MPPT with I	0	0	0	0	0	0	0	0	0	0	0	0	0

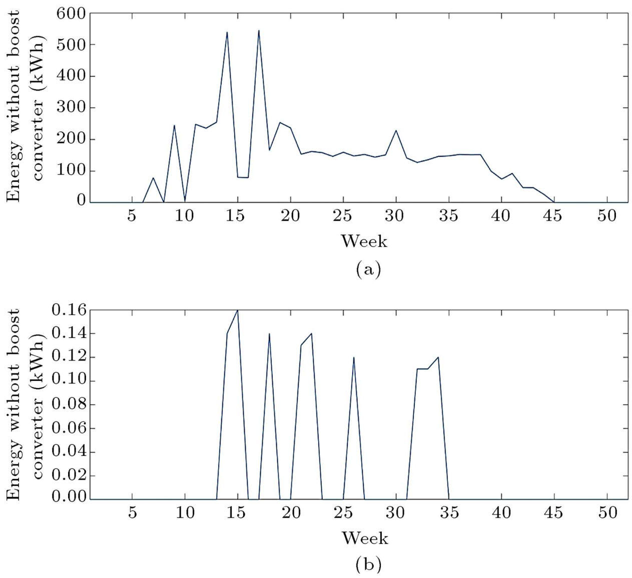

Figure 11. Additional energy output from an 80 kW PV station in kWh in Kabudrahang on different days of the year when: (a) the voltage of the boost converter is reduced from 480 V DC to 240 V DC and (b) the inverter voltage is reduced from 240 V AC to 120 V AC.

equipped only with the inverter was much more than that in the case of the inverter equipped with a boost converter. The converter with a boost converter facilitates capturing a large volume of solar energy in the PV station.

6. Conclusion

The output parameters of PV arrays, voltage-current power, depend on irradiation and ambient temperature at the location of the PV station. Irradiation and temperature affect the energy captured in PV stations directly and inversely, respectively. In this paper, two topologies were investigated in an 80 kW PV station located in Kabudrahang, Iran. The voltages of the boost converter and the inverter were considered 480 V DC and 240 V AC, respectively. Two seasons, summer and autumn, were considered for the simulations. Simulation results showed that in case of low irradiation and high temperature, the decreased output voltage level of PV arrays might be below the cut-off voltage of the inverter. In these conditions, the inverter output voltage was zero and no energy was extracted. Simulation results showed that maximum and minimum values of the extracted output energy were 228.2 kWh and 99.008 kWh during the summer quarter. These values were reduced to 105.52 kWh and 334.985 kWh, respectively, over the autumn quarter. As the output voltage reduced to the cut-off voltage of the inverter, during the summer quarter, no output energy was harvested in the case of applying an inverter in the output of PV arrays. Also, with different converter sets, the output power of the PV station changed accordingly. Because the voltages of the boost converter and the inverter were respectively reduced from 480 V DC to 240 V DC and from 240 V AC to 120 V AC, much more energy would be captured.

Acknowledgment

The authors would like to thank Dr. Abir Chatterjee for his helpful advice and insights which helped conclude this paper.

References

1. Khosrogorji, S., Ghari, H., and Torkaman, H. "Optimal sizing of hybrid WT/PV/diesel generator/battery system using MINLP method for a region in Kerman", *J Scientia Iranica*, **27**(6), pp. 3066–3074 (2020). DOI: 10.24200/SCI.2019.50176.1555

2. Scolari, E., Sossan, F., and Paolone, M. "Photovoltaic model-based solar irradiance estimators: Performance comparison and application to maximum power forecasting", *IEEE Trans. on Sustainable Energy*, **9**(1), pp. 35–44 (2018).

3. Lapeña, O.L-, Penella, M.T., and Gasulla, M. "A new MPPT method for low-power solar energy harvesting", *IEEE Trans. Ind. Electron.*, **57**(9), pp. 3129–3138 (2010).

4. Piegari, L. and Rizzo, R. "Adaptive perturb and observe algorithm for photovoltaic maximum power point tracking", *IET Renew. Power Gener.*, **4**(4), pp. 317–328 (2010).

5. Sossan, F., Kosek, A.M., Martinenas, S., Marinelli, M., and Bindner, H.W. "Scheduling of domestic water heater power demand for maximizing PV self-consumption using model predictive control", *IEEE International Conference on Innovative Smart Grid Technologies (ISGT)*, Lyngby, pp. 1–5 (2013).

6. Luthander, R., Widén, J., Nilsson, D., and Palm, J. "Photovoltaic self-consumption in buildings: A review", *Applied Energy*, **142**, pp. 80–94 (2015).

7. Chatterjee, A., Keyhani, A., and Kapoor, D. "Identification of photovoltaic source model", *IEEE Trans. Energy. Conv.*, **26**(3), pp. 883–889 (2011).

8. Ghaedi, A., Abbaspour, A., Fotuhi-Firuzabad, M., and Parvania, M. "Incorporating large photovoltaic farms in power generation system adequacy assessment", *J. Sci. Iran.*, **21**(3), pp. 924–934 (2014).

9. Markvart, T., *Solar Electricity*, pp. 11–16, Wiley, West Sussex, England (1994).

10. Salcedo-Sanz, S., Casanova-Mateo, C., Munoz-Mari, J., and Camps-Valls, G. "Prediction of daily global solar irradiation using temporal Gaussian processes", *IEEE Geoscience and Remote Sensing Letters*, **11**(11), pp. 1936–1940 (2014).

11. Avila, A., Vizcaya, P.R., and Diez, R. "Daily irradiance test signal for photovoltaic systems by selection from long-term data", *Renewable Energy*, **131**, pp. 755–762 (2019).

12. Laudani, A., Fulginei, F.R., Salvini, A., Carrasco, M., and Mancilla-David, F. "A fast and effective procedure for sensing solar irradiance in photovoltaic arrays", *IEEE 16th International Conference on Environment and Electrical Engineering (EEEIC)*, Florence, Italy, pp. 1–4 (2016).

13. Carrasco, M., Mancilla-David, F., and Ortega, R. "An estimator of solar irradiance in photovoltaic arrays with guaranteed stability properties", *IEEE Transactions on Industrial Electronics*, **61**(7), pp. 3359–3366 (2014).

14. Benali, L., Notton, G., Fouilloy, A., Voyant, C., and Dizene, R. "Solar radiation forecasting using artificial neural network and random forest methods: Application to normal beam, horizontal diffuse and global components", *Renewable Energy*, **132**, pp. 871–884 (2019).

15. Vigni, V.L., Manna, D.L., Sanseverino, E.R., di Dio, V., Romano, P., di Buono, P., Pinto, M., Miceli, R., and Giaconia, C. "Proof of concept of an irradiance estimation system for reconfigurable photovoltaic arrays", *Energies*, **8**(7), pp. 6641–6657 (2015).

16. Zang, H., Cheng, L., Ding, T., Cheung, K.W., Wang, M., Wei, Z., and Sun, G. "Estimation and validation of daily global solar radiation by day of the year-based models for different climates in China", *Renewable Energy*, **135**, pp. 984–1003 (2019).

17. Koo, C., Li, W., Cha, S.H., and Zhang, S. "A novel estimation approach for the solar radiation potential with its complex spatial pattern via machine-learning techniques", *Renewable Energy*, **133**, pp. 575–592 (2019).

18. Gow, J.A. and Manning, C.D. "Development of a photovoltaic arrays model for use in power-electronics simulation studies", *in IEE Proc. Electric Power Appl.*, **146**(2), pp. 193–200 (1999).

19. Banaei, M.R., Ardi, H., Alizadeh, R., and Farakhor, A. "Non-isolated multi-input–single-output DC/DC converter for photovoltaic power generation systems", *IET Power Electron.*, **7**(11), pp. 2806–2816 (2014).

20. Hamzeh Aghdam, F. and Abapour, M. "Reliability and cost analysis of multistage boost converters connected to PV panels", *IEEE Journal of Photovoltaics*, **6**(4), pp. 981–989 (2016).

21. Kumar, J., Agarwal, A., and Agarwal, V. "A review on overall control of DC microgrids", *Journal of Energy Storage*, **21**, pp. 113–138 (2019).

22. Camilo, J.C., Guedes, T., Fernandes, D.A., Melo, J.D., Costa, F.F., and Sguarezi Filho, A.J. "A maximum power point tracking for photovoltaic systems based on monod equation", *Renewable Energy*, **130**, pp. 428–438 (2019).

23. Zerhouni, F.Z., Zerhouni, M.H., Zegrar, M., Benmessaoud, M.T., Tilmatine, A., and Boudghene Stambouli, A. "Modelling polycristallin photovoltaic cells using design of experiments", *J. Sci. Iran.*, **21**(6), pp. 2273–2279 (2014).

24. Biswas, P.P., Suganthan, P.N., Wu, G., and Amaratunga, G.A.J. "Parameter estimation of solar cells using datasheet information with the application of an adaptive differential evolution algorithm", *Renewable Energy*, **132**, pp. 425–438 (2019).

25. Ayang, A., Wamkeue, R., Ouhrouche, M., Djongyang, N., Salom, N.E., Pombe, J.K., and Ekemb, G. "Maximum likelihood parameters estimation of single-diode model of photovoltaic generator", *Renewable Energy*, **130**, pp. 111–121 (2019).

26. Sera, D., Teodorescu, R., and Rodriguez, P. "PV panel model based on datasheet values", In *Proc. IEEE Int. Symp. Electron.*, Vigo, pp. 2392–2396 (2007).

27. Rashid, M.H., *Power Electronics Handbook*, Academic Press (2001).

28. Amir, A., Che, H.S., El Khateb, A., and Nas, A.R. "Comparative analysis of high voltage gain DC-DC converter topologies for photovoltaic systems", *Renewable Energy*, **136**, pp. 1147–1163 (2019).

29. Liu, S., Liu, J., Mao, H., and Zhang, Y. "Analysis of operating modes and output voltage ripple of boost DC-DC converters and its design considerations", *IEEE Trans. Power Electronics*, **23**(4), pp. 1813–1821 (2008).

30. Iqbal, M., *An Introduction to Solar Radiation*, Academic Press, New York, USA, pp. 1–8 (1983).

31. Frohlich, C. and Brusa, R.W. "Solar radiation and its variation in time", *Sol. Phys.*, **74**, pp. 209–215 (1981).

32. Duffie, J.A. and Beckman W., *A Solar Engineering of Thermal Processes*, New York, Wiley (1980).

33. Cooper, P.I. "The absorption of solar radiation in solar stills", *Sol. Energy*, **12**(3), pp. 333–346 (1969).

34. Danandeh, M.A. and Mousavi G.S.M. "Solar irradiance estimation models and optimum tilt angle approaches: A comparative study", *Renewable and Sustainable Energy Reviews*, **92**, pp. 319–330 (2019).

Biographies

Reza Kazemi Golkhandan received his BSc degree from Shahrood University of Technology in 2007, MSc degree from KN. Toosi University of Technology in 2010, and PhD degree from University of Birjand in Iran in 2018. His main research interests include renewable energy systems, microgrids, frequency stability, power electronics, and optimization methods.

Hossein Torkaman is currently an Associate Professor at the Faculty of Electrical Engineering, Shahid Beheshti University, Tehran, Iran. His main research interests include power electronics, electrical machines, and renewable energies.

Ali Keyhani received the BSc, MSc, and PhD degrees from Purdue University, West Lafayette, IN in 1967, 1973, and 1976, respectively. He is currently a Professor of Electrical Engineering at The Ohio State University (OSU), Columbus. He is also the Director of the OSU Electromechanical and Green Energy Systems Laboratory. Dr. Keyhani was the past Chairman of the Electric Machinery Committee of IEEE Power Engineering Society and the past Editor of the IEEE Transaction on Energy Conversion. He was the recipient of The Ohio State University College of Engineering Research Award in 1989, 1999, and 2003.